

Rayleigh-Taylor instability in a two-component Bose-Einstein condensate with rotational symmetryTsuyoshi Kadokura,¹ Tomohiko Aoi,¹ Kazuki Sasaki,¹ Tetsuo Kishimoto,^{1,2,3} and Hiroki Saito¹¹*Department of Engineering Science, University of Electro-Communications, Tokyo JP-182-8585, Japan*²*Center for Frontier Science and Engineering, University of Electro-Communications, Tokyo JP-182-8585, Japan*³*PRESTO, Japan Science and Technology Agency (JST), Saitama JP-332-0012, Japan*

(Received 5 November 2011; published 3 January 2012)

The interfacial instability and subsequent dynamics in a phase-separated two-component Bose-Einstein condensate with rotational symmetry are studied. When the interatomic interaction or the trap frequency is changed, the Rayleigh-Taylor instability breaks the rotational symmetry of the interface, which is subsequently deformed into nonlinear patterns including mushroom shapes.

DOI: [10.1103/PhysRevA.85.013602](https://doi.org/10.1103/PhysRevA.85.013602)

PACS number(s): 03.75.Mn, 67.85.De, 67.85.Fg, 47.20.Ma

I. INTRODUCTION

The Rayleigh-Taylor instability [1–4] (RTI) is the instability of an interface between two fluids in a metastable state. For instance, when a layer of a heavier fluid is laid on a lighter fluid, the system is energetically unfavorable, and the two fluids tend to exchange their positions. However, if the two fluids are immiscible and their interface is flat, the exchange cannot occur without breaking the translation symmetry of the interface. Once an infinitesimal modulation arises on the interface, it exponentially grows due to the RTI, and the interface develops into complicated patterns, such as a mushroom-shaped pattern. Such phenomena are found through nature on a wide scale, ranging from laboratory to astronomical scales. Recently, these kinds of interfacial instabilities have been studied for a system of two-component Bose-Einstein condensate (BEC) [5–8].

The RTI is a symmetry-breaking phenomenon, that is, even when the interface has symmetry (e.g., the translation symmetry of a flat interface and the rotational symmetry of a spherical interface), an infinitesimal modulation grows exponentially, and the symmetry is spontaneously broken. The RTI with rotational symmetry breaking is an important subject, occurring in a variety of systems: e.g., exploding supernovas [9–11], imploding targets in inertial-confinement fusion [12], and collapsing cavitation bubbles [13,14]. In the present paper, we study the rotational-symmetry-breaking RTI in a trapped two-component BEC. Systems of trapped BECs that have so far been proposed for observing the RTI are a tight, pancake-shaped system in which the two components separate into two semicircular shapes [5] and a cigar-shaped system in which a two-component BEC forms a domain structure in the axial direction [6]. In these systems, however, the symmetry-breaking RTI cannot be observed since the relevant symmetry is broken from the initial state due to the inhomogeneity of the trapped systems. In contrast, in the present paper, we propose trapped systems that explicitly show the symmetry-breaking RTI.

We consider a two-component BEC with rotational symmetry in which the two components separate radially and the inner component is surrounded by the shell of the outer component. The interface between the two components has a spherical shape for a spherically symmetric trap and a circular shape for a quasi-two-dimensional axisymmetric trap. If we change a parameter in such a way that the inner component

tends to go out of the outer shell component, the RTI breaks the rotational symmetry of the interface, and the spherical or circular interface is deformed into various patterns. The symmetry-breaking RTI can thus be realized in a trapped BEC.

This paper is organized as follows. Section II provides a formulation of the problem, and Sec. III shows numerical results. Section III A demonstrates the symmetry-breaking RTI and subsequent dynamics for an axisymmetric oblate system. Section III B shows dynamics for a spherically symmetric trap and performs Bogoliubov analysis. Section IV gives conclusions to this study.

II. FORMULATION OF THE PROBLEM

We consider a mixture of two kinds of bosonic atoms with masses m_1 and m_2 confined in trapping potentials V_1 and V_2 , respectively. In the mean-field theory, the system is described by the two-component Gross-Pitaevskii (GP) equation ($j \neq j'$)

$$i\hbar \frac{\partial \psi_j}{\partial t} = \left(-\frac{\hbar^2}{2m_j} \nabla^2 + V_j + g_{jj} |\psi_j|^2 + g_{jj'} |\psi_{j'}|^2 \right) \psi_j, \quad (1)$$

where $g_{jj'} = 2\pi\hbar^2 a_{jj'} (m_j^{-1} + m_{j'}^{-1})$ with $a_{jj'}$ being the s -wave-scattering length between the atoms in components j and j' . The macroscopic wave function ψ_j is normalized as $\int |\psi_j|^2 d\mathbf{r} = N_j$ with N_j being the number of atoms in component j . The two components are miscible for $g_{11}g_{22} > g_{12}^2$ and immiscible for $g_{11}g_{22} < g_{12}^2$.

We solve the three dimensional (3D) GP equation in Eq. (1) numerically, using the pseudospectral method [15]. The initial state is the ground state prepared by the imaginary-time-propagation method in which i on the left-hand side of Eq. (1) is replaced by -1 . We then add a small noise to the initial state as a seed that triggers the RTI. The dynamics do not depend on the initial noise qualitatively.

In the following calculations, we assume a dual-species BEC with ^{85}Rb and ^{87}Rb , where the $|f=2, m_f=-2\rangle$ state of ^{85}Rb is component one and the $|f=1, m_f=-1\rangle$ state of ^{87}Rb is component two. This system has been realized by Papp *et al.* [16] in which controlled phase separation was observed by changing the s -wave-scattering length a_{11} of ^{85}Rb using a magnetic-field Feshbach resonance, which is variable in the range $a_{11} = (50\text{--}900)a_B$ with a_B being the Bohr

radius. Since $a_{22} = 99a_B$ and $a_{12} = 213a_B$, the condition for the phase separation is satisfied for $a_{11} < 458a_B$.

III. NUMERICAL RESULTS

A. Rayleigh-Taylor instability in axisymmetric oblate systems

We first demonstrate the dynamics for an axisymmetric oblate trap $V_j = m_j[\omega_{\perp}^2(x^2 + y^2) + \omega_z^2 z^2]/2$, where $\omega_z \gg \omega_{\perp}$. We assume that the gravitational sag is compensated and that the two components share a common trap center. Figure 1 shows the time evolution of the density and phase profiles of the system, obtained by solving the 3D GP equation in Eq. (1). The initial state is the ground state for $a_{11} = 80a_B$ and $N_1 = N_2$, which has the axisymmetric circular interface between the two components [Fig. 1(a)]. The repulsive interaction of component one (inner) is then gradually increased, and when it exceeds that of component two (outer), the system becomes metastable, i.e., the state in which component one surrounds component two becomes energetically favorable.

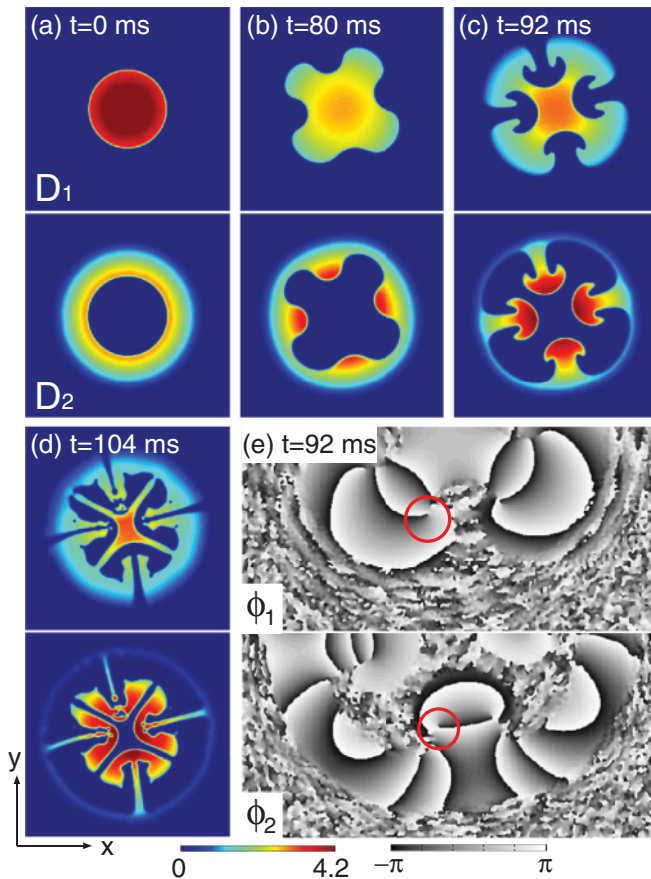


FIG. 1. (Color online) (a)–(d) Dynamics of the column-density profiles $D_1 = \int |\psi_1|^2 dz$ (upper panels) and $D_2 = \int |\psi_2|^2 dz$ (lower panels) in an axisymmetric trap with $(\omega_{\perp}, \omega_z) = 2\pi \times (25, 1250)$ Hz. The scattering length a_{11} is linearly increased from $80a_B$ to $240a_B$ between $t = 0$ and $t = 40$ ms, and after that a_{11} is fixed to $240a_B$. The numbers of atoms are $N_1 = N_2 = 10^5$. The unit of the column density is 10^{12} cm^{-2} . (e) Cross-sectional phase profile $\phi_j = \arg[\psi_j(z=0)]$ of the lower half region of (c). The circles in (e) indicate examples of quantized vortices created under the caps of the mushrooms. The field of view is $65.4 \times 65.4 \mu\text{m}$ in (a)–(d) and $65.4 \times 32.7 \mu\text{m}$ in (e).

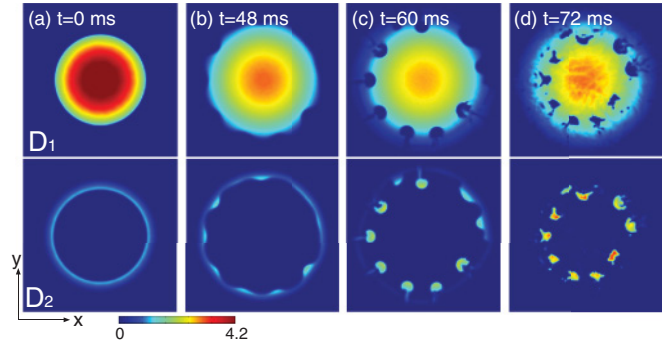


FIG. 2. (Color online) Dynamics of the column-density profiles D_1 and D_2 for $N_1 = 1.8 \times 10^5$ and $N_2 = 2 \times 10^4$. Other parameters are the same as those in Fig. 1.

At $t \simeq 80$ ms, the axisymmetry of the system is broken, and the interface is modulated due to the RTI [Fig. 1(b)]. The modulation of the interface subsequently grows to become a fourfold mushroom shape [Fig. 1(c)]. Quantized vortices are generated under the caps of the mushrooms in both components [circles in Fig. 1(e)]. When the tops of the mushrooms reach the edge or the center of the system, a highly nonlinear pattern is observed [Fig. 1(d)]. The n -fold mushroom shapes with $n \neq 4$ are also observed, where n is larger for a larger final value of a_{11} .

The dynamics also depend on the ratio between the numbers of atoms N_2/N_1 . Figure 2 shows the dynamics for $N_2/N_1 = 1/9$. After the repulsive interaction of component one is increased, the RTI causes modulation at the interface [Fig. 2(b)]. Since N_2 is small, the ring of component two splits into droplets that enter component one, forming small mushrooms [Fig. 2(c)]. The droplets of component two then go toward the center and gather. Their complicated shapes are similar to air bubbles rising in water. The Rayleigh-Taylor “bubbles” as shown in Figs. 1 and 2 have been studied in the context of supernova explosions [10].

B. Rayleigh-Taylor instability in a spherically symmetric system

Next we consider a system confined in a spherically symmetric trap given by $V_j = m_j \omega_j^2 r^2 / 2$ with $r^2 = x^2 + y^2 + z^2$. The initial state is the ground state for $a_{11} = 200a_B$ and $\omega_1 = \omega_2$ in which component two with a spherical shape is surrounded by a shell of component one [Fig. 3(a)]. The trap frequency ω_1 of component one is then increased gradually. The outer component is pushed inward by the increase in the trap frequency, and the RTI is induced at the spherical interface. At $t \simeq 36$ ms, the RTI breaks the rotational symmetry, and the spherical interface is modulated [Figs. 3(b) and 3(d)]. The interface is then deformed into a “mushroom ball” [Fig. 3(e)].

The unstable modes of the interface are estimated by a simple analysis. We assume inviscid, incompressible, and irrotational fluids, and component two of a spherical bubble with radius R is surrounded by component one. The excitation

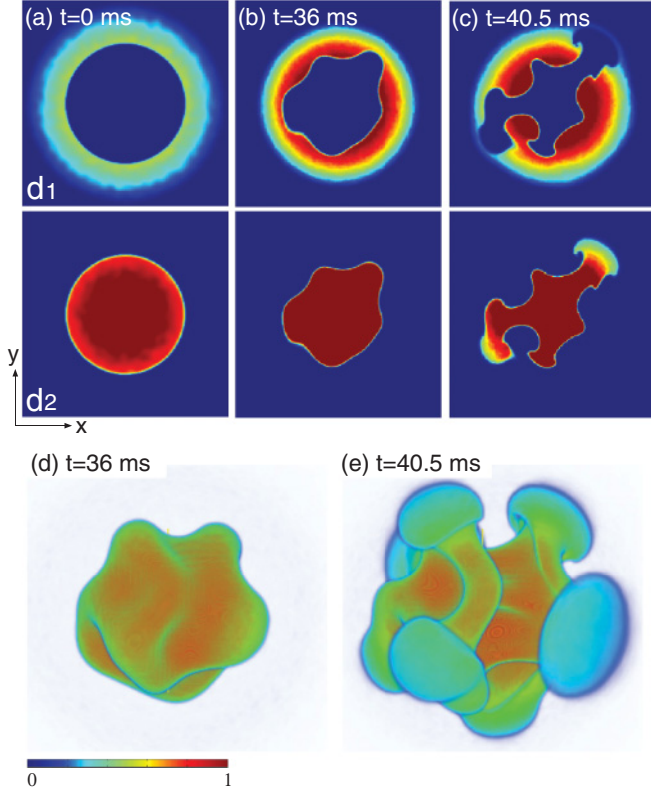


FIG. 3. (Color online) (a)–(c) Dynamics of the cross-sectional density profiles $d_1 = |\psi_1(z=0)|^2$ and $d_2 = |\psi_2(z=0)|^2$ of components one and two and (d), (e) the isodensity surfaces of component two in a spherically symmetric trap with frequency $\omega_1(t=0) = \omega_2 = 2\pi \times 33.3$ Hz. The trap frequency ω_1 is increased such that ω_1^2 is linearly increased from $(\omega_1/\omega_2)^2 = 1$ to 3 between $t = 0$ and $t = 30$ ms, and after that $(\omega_1/\omega_2)^2$ is fixed to 3. The scattering length of component one is $a_{11} = 200a_B$, and the numbers of atoms are $N_1 = N_2 = 5.2 \times 10^6$. The unit of the density is $3.0 \times 10^{14} \text{ cm}^{-3}$. The field of view of each panel is $56.6 \times 56.6 \mu\text{m}$.

frequency Ω of the interfacial mode proportional to the spherical harmonics $Y_l^m(\theta, \phi)$ is given by [17]

$$\Omega^2 = \frac{l(l+1)}{R [lm_1n_1 + (l+1)m_2n_2]} \times \left[n_2f_2 - n_1f_1 + \frac{(l-1)(l+2)\sigma}{R^2} \right], \quad (2)$$

where n_j is the atomic density, f_j is the external force acting on an atom at the interface, and σ is the interfacial-tension coefficient. If Ω is purely imaginary, i.e., the right-hand side of Eq. (2) is negative, the mode is dynamically unstable. Using the expression of σ for a two-component BEC derived in Ref. [18] and $f_j = m_j\omega_j^2 R$, we find that the modes for $1 \leq l \leq 7$ are unstable for the parameters in Fig. 3. [See Fig. 3(d) for the interfacial pattern.]

From Eq. (2), we find that the RTI is induced by an increase in ρ_1 or f_1 or by a decrease in ρ_2 or f_2 . The density ρ_j depends on the interaction: an increase (decrease) in a_{jj} expands (contracts) component j , decreasing (increasing) ρ_j . The force f_j acting on each component can be controlled if the external trapping potential for each component can be controlled independently. The RTI can thus be induced in

several ways: for example, (i) an increase in the scattering length of the inner component, (ii) a decrease in the trap frequency of the inner component, (iii) a decrease in the scattering length of the outer component, or (iv) an increase in the trap frequency of the outer component. The dynamics shown in Figs. 1 and 3 correspond to (i) and (iv), respectively. We have numerically confirmed that the RTI can be observed for all the methods (i)–(iv) for both axisymmetric oblate traps and spherically symmetric traps.

For a more precise understanding of the instability, we perform a Bogoliubov analysis for a spherically symmetric trap. We expand the GP equation in Eq. (1) up to the first order of the deviation $\delta\psi_j(\mathbf{r})$ from the metastable state $\Psi_j(\mathbf{r})$ with spherical symmetry. The excitation mode of the form

$$\delta\psi_j = u_j(r)Y_l^m(\theta, \phi)e^{-i\Omega t} + v_j^*(r)Y_l^{m*}(\theta, \phi)e^{i\Omega t} \quad (3)$$

obeys the Bogoliubov-de Gennes equations ($j \neq j'$)

$$(K_{jl} + V_j - \mu_j + 2g_{jj}\Psi_j^2 + g_{jj'}\Psi_{j'}^2)u_j + g_{jj}\Psi_j^2v_j + g_{jj'}\Psi_j\Psi_{j'}(u_{j'} + v_{j'}) = \hbar\Omega u_j, \quad (4a)$$

$$(K_{jl} + V_j - \mu_j + 2g_{jj}\Psi_j^2 + g_{jj'}\Psi_{j'}^2)v_j + g_{jj}\Psi_j^2u_j + g_{jj'}\Psi_j\Psi_{j'}(u_{j'} + v_{j'}) = -\hbar\Omega v_j, \quad (4b)$$

where μ_j is the chemical potential and

$$K_{jl} = -\frac{\hbar^2}{2m_j} \left[\frac{d^2}{dr^2} + \frac{2}{r} \frac{d}{dr} - \frac{l(l+1)}{r^2} \right]. \quad (5)$$

The wave function Ψ_j is assumed to be real without loss of generality. We numerically diagonalize Eq. (4) to study the stability of the system. If there is a complex frequency Ω , the corresponding mode grows exponentially, and the system is dynamically unstable. Figure 4 shows the imaginary part of the Bogoliubov excitation frequency $\text{Im}\Omega$ as a function of $(\omega_1/\omega_2)^2$. The critical value of $(\omega_1/\omega_2)^2$ above which $\text{Im}\Omega$ rises increases with an increase in l , and above this

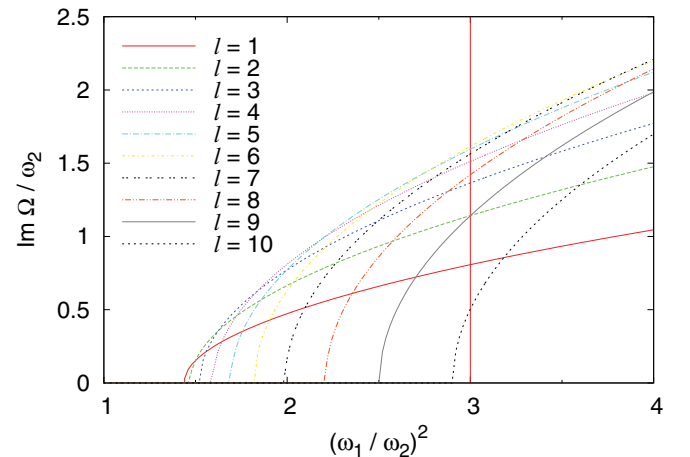


FIG. 4. (Color online) Imaginary part of the Bogoliubov excitation frequency $\text{Im}\Omega$ as a function of $(\omega_1/\omega_2)^2$. The parameters are the same as those in Fig. 3. The modes for $l \leq 10$ are plotted, where l is defined in Eq. (3). The vertical line indicates $(\omega_1/\omega_2)^2 = 3$, corresponding to the parameter in Fig. 3.

critical value of $(\omega_1/\omega_2)^2$, $\text{Im}\Omega$ monotonically increases. At $(\omega_1/\omega_2)^2 = 3$ (the vertical line in Fig. 4), which corresponds to the parameter in Fig. 3, the modes of $l = 1-10$ are unstable. Among these modes, the mode which has the largest $\text{Im}\Omega$ dominates the unstable dynamics. In Fig. 4, since $\text{Im}\Omega$ of the $l = 5-7$ modes are all comparably large, these modes will dominate the unstable dynamics. For these parameters, the analytic expression in Eq. (2) estimates that the modes of $l = 1-7$ are unstable whereas the modes of $l = 1-10$ are unstable in Fig. 4. The difference is attributed to the assumptions of incompressibility and inhomogeneous density distribution in Eq. (2) and the ambiguity in the interfacial-tension coefficient σ for a trapped system.

IV. CONCLUSIONS

In conclusion, we have investigated the interfacial instabilities and subsequent dynamics in phase-separated two-component BECs. Since the initial state has rotational symmetry, the symmetry-breaking nature of the RTI can specifically be observed in this system. We have demonstrated the RTI and ensuing dynamics for an axisymmetric oblate trap (Figs. 1

and 2) and a spherically symmetric trap (Fig. 3), and the mushroom-shaped patterns are observed for both systems, breaking the rotational symmetry. We performed a Bogoliubov analysis for the spherically symmetric system and obtained an unstable spectrum (Fig. 4).

In view of the recent development in the control of two-component BECs [16,19,20], we expect that not only the phenomena predicted in the present paper but also other theoretical predictions [5-8,21-24] concerning interfacial instabilities in two-component BECs will be realized in experiments in the near future.

ACKNOWLEDGMENTS

This work was supported by Grants-in-Aid for Scientific Research (No. 22340116, No. 23540464, and No. 23740307) from the Ministry of Education, Culture, Sports, Science and Technology of Japan and the Japan Society for the Promotion of Science. T.K. acknowledges the Special Coordination Funds for Promoting Science and Technology from the Japan Science and Technology Agency.

-
- [1] Lord Rayleigh, *Proc. London Math. Soc.* **14**, 170 (1883).
 - [2] G. I. Taylor, *Proc. R. Soc. London, Ser. A* **201**, 192 (1950).
 - [3] D. J. Lewis, *Proc. R. Soc. London, Ser. A* **202**, 81 (1950).
 - [4] For example, see S. Chandrasekhar, *Hydrodynamic and Hydro-magnetic Stability* (Clarendon Press, Oxford, 1961), Chap. 10.
 - [5] K. Sasaki, N. Suzuki, D. Akamatsu, and H. Saito, *Phys. Rev. A* **80**, 063611 (2009).
 - [6] S. Gautam and D. Angom, *Phys. Rev. A* **81**, 053616 (2010).
 - [7] A. Bezett, V. Bychkov, E. Lundh, D. Kobaykov, and M. Marklund, *Phys. Rev. A* **82**, 043608 (2010).
 - [8] D. Kobaykov, V. Bychkov, E. Lundh, A. Bezett, V. Akkerman, and M. Marklund, *Phys. Rev. A* **83**, 043623 (2011).
 - [9] A. Burrows, *Nature (London)* **403**, 727 (2000).
 - [10] V. Bychkov, M. V. Popov, A. M. Oparin, L. Stenflo, and V. M. Chechetkin, *Astron. Rep.* **50**, 298 (2006).
 - [11] W. H. Cabot and A. W. Cook, *Nat. Phys.* **2**, 562 (2006).
 - [12] H. Sakagami and K. Nishihara, *Phys. Rev. Lett.* **65**, 432 (1990).
 - [13] M. S. Plesset, *J. Appl. Phys.* **25**, 96 (1954).
 - [14] M. P. Brenner, D. Lohse, and T. F. Dupont, *Phys. Rev. Lett.* **75**, 954 (1995).
 - [15] W. H. Press, S. A. Teukolsky, W. T. Vetterling, and B. P. Flannery, *Numerical Recipes*, 3rd ed. (Cambridge University Press, Cambridge, 2007), Sec. 20.7.
 - [16] S. B. Papp, J. M. Pino, and C. E. Wieman, *Phys. Rev. Lett.* **101**, 040402 (2008).
 - [17] H. Lamb, *Hydrodynamics*, 6th ed. (Dover, New York, 1945), Sec. 275.
 - [18] B. Van Schaeybroeck, *Phys. Rev. A* **78**, 023624 (2008); **80**, 065601 (2009).
 - [19] K. M. Mertes, J. W. Merrill, R. Carretero-González, D. J. Frantzeskakis, P. G. Kevrekidis, and D. S. Hall, *Phys. Rev. Lett.* **99**, 190402 (2007).
 - [20] S. Tojo, Y. Taguchi, Y. Masuyama, T. Hayashi, H. Saito, and T. Hirano, *Phys. Rev. A* **82**, 033609 (2010).
 - [21] H. Saito, Y. Kawaguchi, and M. Ueda, *Phys. Rev. Lett.* **102**, 230403 (2009).
 - [22] H. Takeuchi, N. Suzuki, K. Kasamatsu, H. Saito, and M. Tsubota, *Phys. Rev. B* **81**, 094517 (2010).
 - [23] N. Suzuki, H. Takeuchi, K. Kasamatsu, M. Tsubota, and H. Saito, *Phys. Rev. A* **82**, 063604 (2010).
 - [24] K. Sasaki, N. Suzuki, and H. Saito, *Phys. Rev. A* **83**, 053606 (2011).